

# Measurements of the Electric Polarizabilities of the Alkalis Using the $E$ - $H$ Gradient Balance Method\*†

ARTHUR SALOP,‡ EDWARD POLLACK, AND BENJAMIN BEDERSON

*Department of Physics, New York University, University Heights, New York, New York*

(Received June 12, 1961)

The atomic beam  $E$ - $H$  gradient balance method has been used to measure the polarizabilities of the alkali atoms. In this method, congruent electric and magnetic fields are established in the same region of space by applying a potential difference to pole pieces of high permeability which are insulated from their magnet yoke. The condition that atoms in a particular magnetic substate suffer no deflection in such a field region is  $\alpha E \partial E / \partial z = \mu_{\text{eff}} \partial H / \partial z$ , where  $\alpha$  is the atomic polarizability,  $\mu_{\text{eff}}$  is the effective magnetic moment in the field  $H$ , and  $\partial E / \partial z$  and  $\partial H / \partial z$  are the transverse components of the gradients of the electric and magnetic fields, respectively. Because of the congruence of the  $E$  and  $H$  fields,  $(\partial E / \partial z) / E = (\partial H / \partial z) / H$ , and therefore  $\alpha = \mu_{\text{eff}} H / E^2$  when the balance condition is satisfied. The determination of  $\alpha$  is therefore independent of the velocity distribution in the beam, the field

gradients and the apparatus geometry (except where it enters into the calculation of the electric field). The magnetic field  $H$  is readily measured by making use of the convenient alkali zero moments. In these experiments, absolute accuracy for the  $\alpha$ 's is limited by the uncertainty in the determination of  $E$ , which is calculated from a knowledge of the applied voltage and the gap geometry.

The results in units of  $10^{-24}$  cm<sup>3</sup> are: Li,  $20 \pm 3.0$ ; Na,  $20 \pm 2.5$ ; K,  $36.5 \pm 4.5$ ; Rb,  $40 \pm 5.0$ ; Cs,  $52.5 \pm 6.5$ . These are considerably higher than the values obtained in early beam experiments using electrostatic deflection techniques. They are, however, in fairly good agreement with the recent calculations of Dalgarno and Kingston and with other theoretical determinations of alkali polarizabilities.

## INTRODUCTION

DURING the 1930's, Scheffers and Stark conducted a series of experiments in which they measured the polarizabilities of lithium, potassium, cesium,<sup>1</sup> and atomic hydrogen<sup>2</sup> by passing beams of atoms through a strong inhomogeneous electric field. A beam atom in such a field experiences a transverse force equal to the product of the induced dipole moment  $\alpha E$ , and the component of the gradient of the electric field in the transverse direction, where  $\alpha$  is the atomic polarizability and  $E$ , the electric field strength. The polarizabilities were obtained from an analysis of the resulting deflection patterns. The basic shortcoming of this method is the smearing out of the deflection pattern due to the distribution of velocities in the beam. An elaborate analysis is required to obtain a polarizability value. The determination depends critically upon precise knowledge of the velocity distribution, apparatus geometry, and the beam shape, and it becomes very difficult to obtain good precision. Recent calculations of alkali polarizabilities by Sundbom,<sup>3</sup> Dalgarno and Kingston,<sup>4</sup> and Parkinson<sup>5</sup> have not been in agreement with the Scheffers and Stark values. Furthermore, the early semi-empirical estimates by Fues,<sup>6</sup> based on the optical Stark effect, ranged from over 100% higher (for lithium) to 35% higher (for potassium). Haun and Zacharias<sup>7</sup>

have examined the effect of an electric field on the hyperfine structure of Cs<sup>133</sup>. Subsequently, Mizushima<sup>8</sup> has shown that their results are consistent with a cesium polarizability considerably higher than the Scheffers and Stark value.

In the polarizability measurements described in this paper, a new atomic beam method is used in which the disturbing effect of the velocity distribution is essentially eliminated. Furthermore, in this method, the results turn out to be independent of specific values of the field gradient and, with the exception of the electric field determination, independent of the apparatus geometry. We call this technique the " $E$ - $H$  Gradient Balance Method."<sup>9</sup>

Concurrently with this work, Chamberlain and Zorn, at Yale, have made measurements of the alkali polarizabilities using a modified electrostatic deflection technique. They will present their results in a forthcoming publication.

## EXPERIMENTAL METHOD

An alkali beam is produced and detected by conventional means.<sup>10</sup> The beam passes through a region of strong, transverse inhomogeneous electric field. The electrodes which produce this field are made of high permeability soft iron, and also act as the pole pieces of a magnet. They are insulated from the yoke which is placed outside the vacuum system. The electric and magnetic fields between the electrodes should be almost perfectly congruent, provided saturation effects in the iron are avoided. That is, the electric field should be proportional to and in the same direction as the magnetic field at every point in this region.

The individual beam atom traversing the field region

\* Supported by the U. S. Office of Naval Research.

† For a preliminary report of this work, see Bull. Am. Phys. Soc. 5, 381 (1960).

‡ From part of a thesis submitted by A. Salop in partial fulfillment of the requirements for the degree of Doctor of Philosophy, Department of Physics, New York University, New York, New York.

<sup>1</sup> H. Scheffers and J. Stark, Phys. Z. 35, 625 (1934).

<sup>2</sup> H. Scheffers and J. Stark, Phys. Z. 37, 217 (1936).

<sup>3</sup> M. Sundbom, Arkiv Fysik 13, 539 (1958).

<sup>4</sup> A. Dalgarno and A. E. Kingston, Proc. Phys. Soc. (London) A73, 455 (1959).

<sup>5</sup> D. Parkinson, Proc. Phys. Soc. (London) A75, 169 (1960).

<sup>6</sup> E. Fues, Z. Physik 82, 536 (1933).

<sup>7</sup> R. D. Haun, Jr. and J. R. Zacharias, Phys. Rev. 107, 107 (1957).

<sup>8</sup> M. Mizushima (private communication).

<sup>9</sup> B. Bederson, J. Eisinger, K. Rubin, and A. Salop, Rev. Sci. Instr. 31, 852 (1960).

<sup>10</sup> N. F. Ramsey, *Molecular Beams* (Oxford University Press, New York, 1956).

experiences transverse forces due to both the inhomogeneous electric and magnetic fields. The magnetic force is  $\mu_{\text{eff}}(\partial H/\partial z)$ , where  $\mu_{\text{eff}}$  is the effective magnetic moment in the direction of the field, and  $\partial H/\partial z$  is the transverse component of the gradient of the magnitude of the magnetic field. The electric force is  $\alpha E(\partial E/\partial z)$ , where  $\alpha E$  is the induced electric dipole moment and  $\partial E/\partial z$  is the transverse component of the gradient of the magnitude of the electric field.

For certain magnetic substates (those for which  $\mu_{\text{eff}}$  is negative in the sense of being opposite to the magnetic field direction), it is possible to make the magnetic and electric forces equal and opposite. Thus, when the forces are balanced,

$$\alpha E(\partial E/\partial z) = \mu_{\text{eff}}(\partial H/\partial z), \quad (1)$$

where in this equation,  $\mu_{\text{eff}}$  represents the magnitude of the effective moment. Now, in the gap region,  $\partial E/\partial z = CE$  and  $\partial H/\partial z = CH$ , where  $C$  is a geometry factor which, because of the  $E$ - $H$  congruence, is the same for both fields. Using these relationships in Eq. (1), we obtain for a particular magnetic substate when the  $E$ - $H$  balance prevails,

$$\alpha = \mu_{\text{eff}} H / E^2. \quad (2)$$

For the alkalis,  $\mu_{\text{eff}}$  is a known function of  $H$ , and therefore the determination of  $\alpha$  reduces to the problem of obtaining  $E$  and  $H$  at the balance condition. The method is therefore independent of the velocity distribution in the beam, the specific values of the field gradients, and the apparatus geometry (except where it enters into the calculation of the electric field).

Generally, in performing the measurements, the magnetic field was fixed at some convenient value, which could be accurately measured by the use of the "zero moment" technique.<sup>11</sup> The electric field was then varied until the balance condition was achieved for a particular magnetic substate, whereupon a clearly defined beam intensity maximum was observed at the detector. The electric field may, of course, be calculated to a fair degree of accuracy from a knowledge of the electrode geometry and the applied voltage. In practice, it was the uncertainty associated with the determination of the electric field at the position of the beam which limited the accuracy of our results.

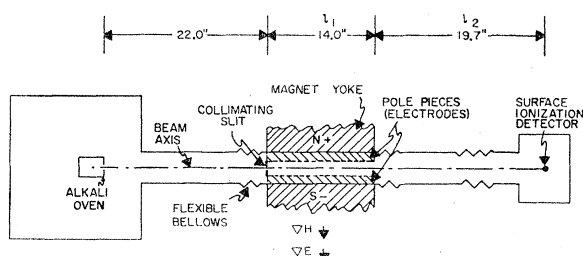


FIG. 1. Schematic diagram of the atomic beam apparatus.

<sup>11</sup> V. W. Cohen, Phys. Rev. 46, 713 (1934).

The balance condition is valid only for beams of infinitesimal width. For beams of finite width, the condition cannot in general be simultaneously satisfied over the full beam. It can be shown, however, that for the beam widths used in this experiment, the broadening effect is quite small (see Appendix).

## APPARATUS

A schematic diagram of the beam apparatus is shown in Fig. 1. The vacuum system consists of a large cylindrical oven chamber, a long, narrow main chamber made up of several easily demountable components, and a small detector chamber. The oven chamber is pumped by an Edwards 9 in. type F903 oil diffusion pump, with associated refrigerated baffling. The main chamber is pumped by two Litton type PB oil diffusion pumps, each possessing a water baffle and a bakeable charcoal

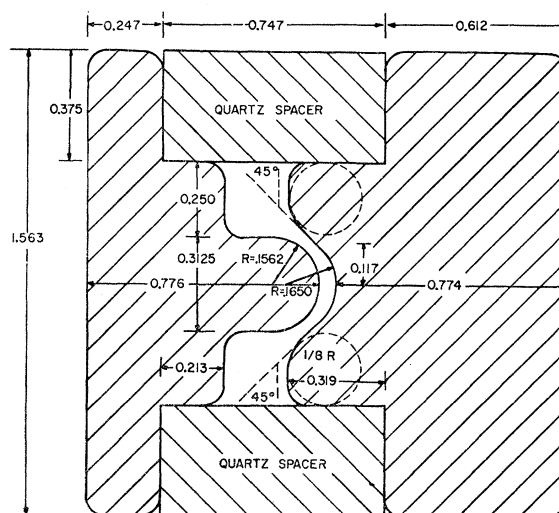


FIG. 2. Cross section of inhomogeneous field pole pieces (electrodes) listing all relevant dimensions in inches.

baffle. In normal operation, these pumps maintain a pressure in the entire system of about  $10^{-6}$  mm Hg.

The sources were conventional alkali ovens<sup>10</sup> machined from nickel for cesium, rubidium, potassium, and sodium, and from molybdenum for lithium. The oven slit was 0.0025 in. wide and 0.125 in. high.

The detector was a conventional surface ionization hot wire detector of 0.002 in. diam. For cesium, rubidium, and potassium, the detecting element was a Pt-W wire.<sup>12</sup> For sodium, pure tungsten was used, which was oxidized by heating under forepressure vacuum before a run. For lithium, the Pt-W alloy was used with continuous oxygenation from a carefully controlled oxygen spray mounted above the hot wire.

The entire detector chamber was mounted on a universal table (actually a milling machine attachment)

<sup>12</sup> 92% Pt-8% W, procured from the Sigmund Cohn Corporation, Mount Vernon, New York, as alloy 479.

with a precision feed screw, so that it could be moved in a direction transverse to the beam path. The chamber was connected to the rest of the system through a short section of flexible metal hose, enabling the detector to be translated over distances of up to one inch off the beam axis. A dial gauge was used to measure the relative detector position to within 0.0005 in. The ion current was measured by a Keithley model 610 electrometer used in conjunction with an automatic recorder.

The inhomogeneous field magnet (or electrode system) was machined from Armco iron and heat treated in accordance with standard procedure. Figure 2 is a cross-sectional view showing the contours of the pole pieces, which are included within the vacuum system. The pole pieces are 14 inches long, and are shaped to conform with magnetic equipotential surfaces which result from a two wire configuration. Two precision ground quartz spacers, also 14 in. in length, fit between the pole pieces and determine the gap spacing. The

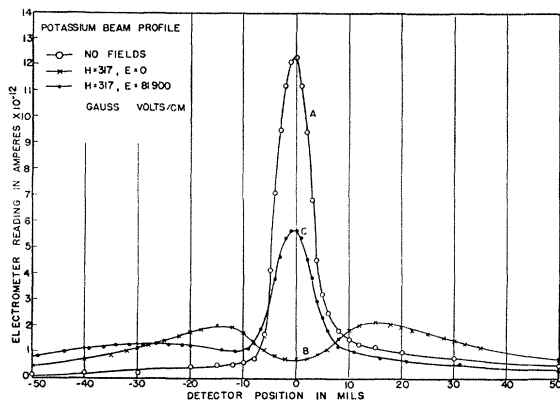


FIG. 3. Qualitative demonstration of  $E$ - $H$  field congruency, showing potassium beam profile under the conditions: A. No fields; B. magnetic field and no electric field; C. magnetic and electric fields at balance condition.

entire assembly fits snugly into a 15-in. long rectangular cross section glass tube with precise inner dimensions which also serves as the vacuum envelope. (The yoke is positioned externally to the glass tube.) Located just before the entrance to the field region is the 0.002 in. wide collimating slit placed so that the beam can be made to run parallel to the pole pieces at a distance  $1.2a$  from the line joining the equivalent two wires, where  $2a$  is the distance between these equivalent wires. The beam is limited in height to 0.060 in. in order to minimize the effect of the variation of field and gradient in the vertical plane.

Since these pole pieces also serve as electrodes for an inhomogeneous electric field, precautions were necessary to prevent high voltage breakdowns. The contour curvatures were made as gentle as possible, and the pole face surfaces were highly polished.

The high voltage supply was a Spellman model lab 60 PN having a range of 0-60 kv. A Sensitive Research

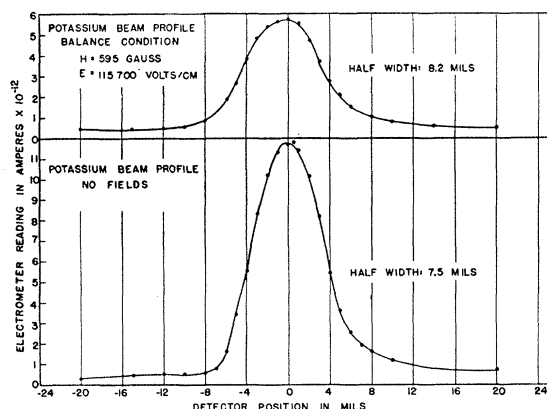


FIG. 4. Quantitative demonstration of  $E$ - $H$  field congruency, showing comparison of undeflected beam profile and balance peak profile for potassium in a "strong" magnetic field.

type ESHMIX electrostatic voltmeter was used to measure the applied voltages. The instrument calibration was checked at the National Bureau of Standards.

The exciting coil for the magnetic field, consisting of 2400 turns of No. 16 Formvar coated copper wire, was driven by a Kepco SC 36-1M power supply having a range of 0-36 v at one amp. With a one-amp coil current, the magnetic field at the beam position was about 4500 gauss. The maximum magnetic field required during the experiment was only about 3000 gauss. Both the electric and magnetic fields were capable of being automatically varied at a slow rate for continuous recording purposes.

## EXPERIMENTAL PROCEDURES AND RESULTS

### 1. Field Congruency Tests

Several checks were made to test the general performance of the balance method, and particularly the assumption of field congruency. The three curves of Fig. 3 demonstrate the operation of the balance method. Curve A shows a potassium beam profile taken at zero  $E$  and  $H$  fields. Curve B shows a profile taken at  $E=0$ ,  $H=317$  gauss, i.e., a typical Stern-Gerlach pattern, showing two velocity-broadened peaks at either side of the beam axis. (The applied field is large enough so that the electron and nuclear spins are essentially decoupled, i.e.,  $\mu_{\text{eff}} \approx \pm \mu_0$ .) Curve C shows a profile taken at  $E=81,900$  v/cm and  $H=317$  gauss, which represents a balance condition for this case. The left-hand peak ( $\mu \approx +\mu_0$ ) has shifted further to the left and has been further broadened by the velocity distribution. The right-hand peak ( $\mu \approx -\mu_0$ ) has shifted to the origin and has sharpened up so as to closely approximate the original beam shape. It is apparent that, at least qualitatively, the broadening effect of the velocity distribution has been eliminated for this state.

The same procedure was followed at a higher field in order to obtain a quantitative check on the field congruency. Figure 4 shows an undeflected beam profile

for potassium and a balance peak profile at  $E=115\,700$  v/cm and  $H=595$  gauss. (The deflection, in the transverse plane of the detector, of atoms having the most probable velocity in a magnetic field of 595 gauss is about 0.010 in.) The half-width of the original beam is 0.0075 in., and the half-width of the balanced peak is 0.0082 in. The maximum intensity of the balance peak is slightly less than half that of the full beam. The slight broadening of the balance peak is consistent with the assumption of perfect congruence and perfect balance at the center of a beam of finite width. However, it can only be stated for certain, that all unbalanced forces, including the effects due to incongruency, the finite beam width, fringing fields, etc., altogether produce a 9% broadening of the original beam for this case. It is seen that the fields are indeed congruent to a fairly high degree of approximation.

## 2. Cesium Measurements

Balance measurements for cesium (as for the other alkalis) were made in a number of ways and the experimental runs were repeated over an extended period of time. Figure 5 shows the effective magnetic moments of an  $I=\frac{7}{2}$ ,  $J=\frac{1}{2}$  atom ( $\text{Cs}^{133}$ ) for the various magnetic substates, plotted as a function of the dimensionless parameter  $x \approx g_J \mu_0 H / \Delta W$ , where  $g_J$  is the atomic  $g$  factor, and  $\Delta W$  the zero field hyperfine energy separation. In a typical experiment, the magnetic field was adjusted to one of the zero-moment fields,<sup>13</sup> for example, the second zero-moment field of  $\text{Cs}^{133}$ . With reference to Fig. 5, if a vertical line is drawn downward from the point on the  $x$  axis corresponding to the second zero

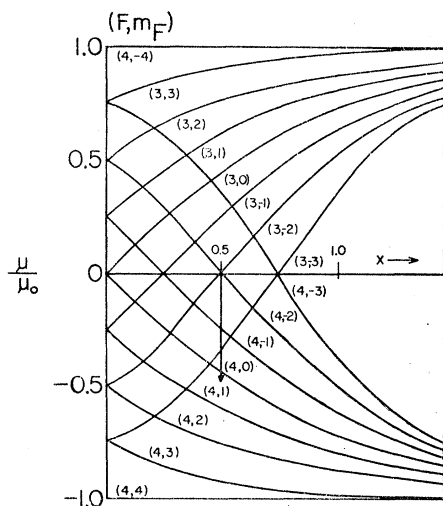


FIG. 5. The variation of effective magnetic moments with dimensionless parameter  $x$  (proportional to  $H$ ) for an  $I=\frac{7}{2}$ ,  $J=\frac{1}{2}$  atom ( $\text{Cs}^{133}$ ).

<sup>13</sup> Alkali isotopes with odd half-integral nuclear spins have zero-moment states at zero magnetic fields. For such isotopes, we refer to the first zero moment as that one which occurs at the lowest nonzero value of magnetic field.

moment, the line intersects the various magnetic substate curves. If the applied voltage is now turned on and gradually increased, the zero-moment atoms will be deflected away from the detector, and one by one, the balance condition will then be realized for each of the negative effective moment substates, resulting in the appearance of sharp maxima in the detector current. In principle, seven balance peaks should be observed at the cesium second zero-moment field, but because of high voltage breakdowns, the applied voltage was limited to a maximum of about 18 000 v and only three substates could be observed, corresponding to  $(4, -1)$ ,  $(3, -3)$ , and  $(4, 0)$ .

Typical recorder traces of beam intensity vs applied voltage taken automatically with both increasing and decreasing voltage are shown in Fig. 6. The appreciable differences in the widths and intensities of the three balance peaks observed are attributable to the differences in focusing action of the fields for these three substates (see Appendix).

Data were taken at the second zero-moment field of  $\text{Cs}^{133}$ , ( $H=1634$  gauss), at the third zero-moment field ( $H=2451$  gauss), and at a field intermediate to the second and third zero moments, with  $H$  determined using an interpolation technique.

The data obtained for cesium and the resulting polarizability determinations are presented in condensed form in Table I together with similar data for rubidium, potassium, and sodium. The values listed for the electric fields represent, in general, averages obtained from several measurements of the applied voltage at a balance peak taken with both increasing and decreasing voltage scans. The averages of the "up" and "down" balance condition voltages were used in order to eliminate time lag errors.

The final value of  $\alpha$  for  $\text{Cs}^{133}$  was obtained as an average of 22 independent runs taken over a period of several months. In obtaining the final value of  $\alpha$ , the determinations at the zero moments were given twice the weight of those made at the intermediate field. A conservative estimate of the total error in the polarizability average (including possible systematic errors)

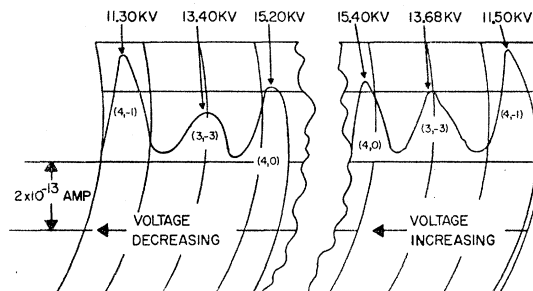


FIG. 6. Recorder traces of the balance peaks of three  $\text{Cs}^{133}$  substates at a magnetic field of 1634 gauss, corresponding to the second  $\text{Cs}^{133}$  zero moment.

is  $\pm 12\%$ . (See section on Discussion of Results.) We find

$$\alpha(\text{Cs}) = (52.5 \pm 6.5) \times 10^{-24} \text{ cm}^3.$$

### 3. Rubidium Measurements

Measurements on various substates of  $\text{Rb}^{85}$  were made at the second zero moment of  $\text{Rb}^{85}$  ( $H=722$  gauss), the zero moment of  $\text{Rb}^{87}$  (1221 gauss), and at an intermediate field value ( $U=972$  gauss). Figure 7 shows the ratios  $\mu_{\text{eff}}/\mu_0$  for the ten negative substates of  $\text{Rb}^{85}$  ( $I=\frac{5}{2}$ ) and  $\text{Rb}^{87}$  ( $I=\frac{3}{2}$ ), including the zero moment substate of  $\text{Rb}^{85}$ , at  $H=722$  gauss. At this field value, it was convenient to perform the balance measurements on the  $\text{Rb}^{85}$  (3,0) substate, since it is well separated here in  $\mu_{\text{eff}}$  from its neighbors. The  $\text{Rb}^{85}$  (3,3),  $\text{Rb}^{87}$  (2,2),

TABLE I.  $E$ - $H$  gradient balance measurements for cesium, rubidium, potassium, and sodium.

Alkali isotope	Run No.	Magnetic substate ( $F, M_F$ )	Magnetic field (gauss)	Effective magnetic moment (Bohr magnetons)	Electric field <sup>a</sup> (esu)	Electric polarizability ( $10^{-24} \text{ cm}^3$ )
$\text{Cs}^{133}$	1	(4, -1)	1634	0.250	266.9	53.2
	2				267.3	53.0
	3				266.9	53.2
	4				271.2	51.5
	5				272.4	51.1
	6	(3, -3)	1634	0.354	318.9	52.7
	7				314.8	54.1
	8				319.9	52.4
	9				323.7	51.2
	10				360.4	52.1
	11	(4, 0)	1634	0.447	362.6	51.5
	12				365.4	50.7
	13				366.2	50.5
	14				344.2	53.1
	15				343.3	53.4
	16	(4, -2)	2451	0.277	345.2	52.8
	17				345.6	52.7
	18				345.4	52.7
	19				347.3	52.2
	20				286.7	53.7
	21	(4, -2)	2247	0.212	285.2	54.2
	22				292.6	51.6
$\text{Rb}^{85}$	1	(3, 0)	722	0.554	307.9	39.1
	2				308.9	38.9
	3				305.8	39.7
	4				305.3	39.8
	5				303.3	40.3
	6				308.6	38.9
	7	(3, -2)	1221	0.524	382.6	40.5
	8				387.9	39.4
	9				386.0	39.8
	10				383.8	40.3
	11	(3, 0)	972	0.668	386.0	39.8
	12				382.6	41.1
	13				332.3	41.9
	14				337.5	40.6
	15				336.1	40.9
	16	(3, -1)	972	0.513	336.6	40.8
	17				336.6	40.8
$\text{K}^{39}, \text{K}^{41}$	1	b	722	0.985 <sup>c</sup>	427.2	36.1
	2				429.9	35.7
	3				428.0	36.8
	4				427.8	36.8
	5				401.5	36.9
	6				385.3	36.8
	7				400.3	37.3
	8				401.0	37.1
	9				417.6	35.8
$\text{Na}^{23}$	1	(2, 0)	316	0.447	256.1	20.0
	2	(2, 1)	316	0.756	333.7	19.9
	3	(2, -1)	592	0.450	348.0	20.4
	4	(2, -1)	642	0.511	389.6	20.0
	5	(2, -1)	672	0.544	407.0	20.5

<sup>a</sup> Each value represents, in general, an average, corresponding to several up and down sweeps of the applied voltage.

<sup>b</sup> The measurements for potassium were made in strong magnetic fields such that  $|\mu_{\text{eff}}/\mu_0| \approx 1$  for all of the magnetic substates.

<sup>c</sup> Each value represents a weighted average over the various magnetic substates (having negative effective moments) of  $\text{K}^{39}$  and  $\text{K}^{41}$ .

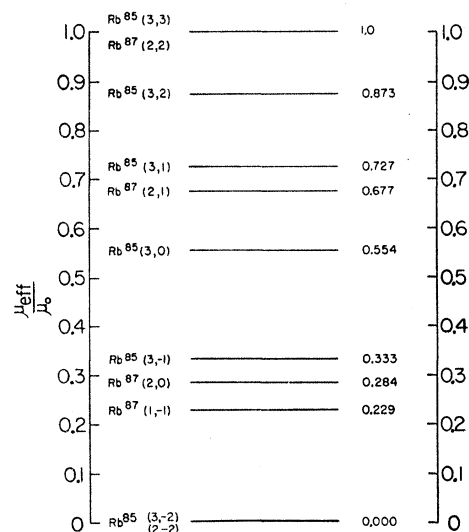


Fig. 7. Effective moments of  $\text{Rb}^{85}$  and  $\text{Rb}^{87}$  substates at a magnetic field corresponding to the second zero moment of  $\text{Rb}^{85}$  (722 gauss).

and  $\text{Rb}^{85}$  (3,2) substates required voltages higher than the sparking potential to obtain balance. At the  $\text{Rb}^{87}$  zero moment field, the balance measurements were made on the  $\text{Rb}^{85}$  (3, -2) substate, for similar reasons. Figure 8 shows a recorder trace of the balance substates  $\text{Rb}^{85}$  (3,0),  $\text{Rb}^{85}$  (3,1), and  $\text{Rb}^{87}$  (2,1) taken at  $H=722$  gauss. Note that the latter two states are not resolved because their  $\mu_{\text{eff}}$ 's are insufficiently separated. (See Fig. 7) In obtaining the final value for  $\alpha$ , the determinations at the zero moments were given twice the weight of those made at the intermediate field. An estimate of the overall error, including possible systematic errors, is  $\pm 12\%$ . We find

$$\alpha(\text{Rb}) = (40.0 \pm 5.0) \times 10^{-24} \text{ cm}^3.$$

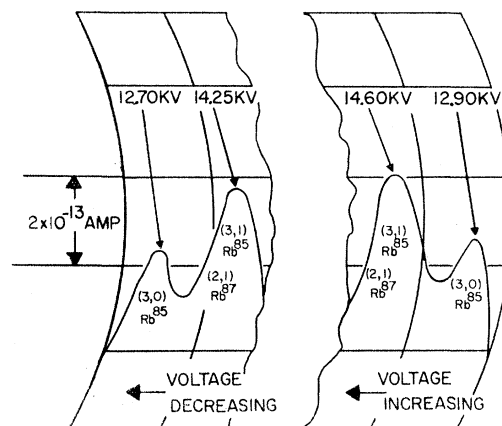


Fig. 8. Recorder traces of the balance peaks of three Rb substates at a magnetic field of 722 gauss, corresponding to the second zero moment of  $\text{Rb}^{85}$ . Note that the (3,1)  $\text{Rb}^{85}$  and (2,1)  $\text{Rb}^{87}$  substates are unresolved.

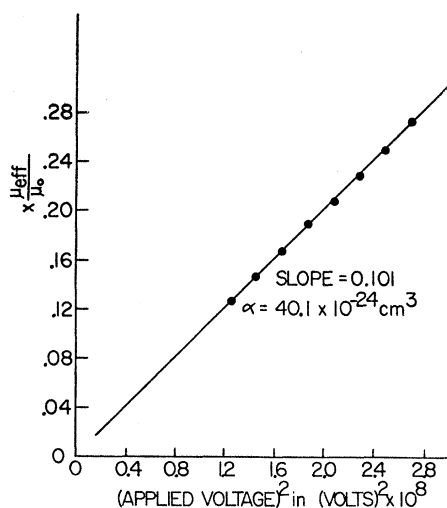


FIG. 9. Plot showing the linear relation between  $\mu_{\text{eff}} H$  and  $E^2$  at the balance condition for the (2,1)  $\text{Rb}^{87}$  substate for magnetic fields above 1221 gauss. (Actually, the proportional quantities  $x\mu_{\text{eff}}/\mu_0$  and  $V^2$  are plotted.) The measured slope of such a curve yields an independent determination of  $\alpha$ .

An additional demonstration of the proper operation of the  $E$ - $H$  gradient balance method was the expected linearity between  $\mu_{\text{eff}} H$  and  $E^2$ . Experimental curves were obtained for particular substates of both  $\text{Rb}^{87}$  and  $\text{Cs}^{133}$  which showed this linearity over a wide range of magnetic fields. A typical curve for the (2,-1) substate of  $\text{Rb}^{87}$  for a range of magnetic field values above that of the zero moment of  $\text{Rb}^{87}$  is plotted in Fig. 9. Actually, it was convenient to plot  $\mu_{\text{eff}} x/\mu_0$  (proportional to  $\mu_{\text{eff}} H$ ) vs  $V^2$  (proportional to  $E^2$ ). The slope of such a curve is proportional to the polarizability, and using this technique, the polarizability of  $\text{Rb}^{87}$  was found to agree within experimental error with that of the previously determined  $\text{Rb}^{85}$  value. (The balance measurements at the zero moment fields were all made on  $\text{Rb}^{85}$  since the apparatus was unable to resolve completely any of the  $\text{Rb}^{87}$  substates.)

#### 4. Potassium Measurements

Because of the relatively small hyperfine separations for the potassium isotopes, the region of intermediate coupling, where the  $\mu_{\text{eff}}$ 's of the various substates are widely separated, occurs at very low field values (<150 gauss). The apparatus resolving power at these low fields is insufficient to separate the substates. Instead, the balance technique was employed in the high field region where  $\mu_{\text{eff}} \pm \mu_0$  for all the substates. The data, which are presented in Table I, were taken at, or near, the second  $\text{Rb}^{85}$  zero moment magnetic field. An extrapolation technique was employed to determine the magnetic fields using the rubidium zero moments as reference points. Note that the  $\mu_{\text{eff}}$  values for potassium represent the weighted averages over the eight negative substates of  $\text{K}^{39}$  and  $\text{K}^{41}$ . The over-all error is again

estimated to be  $\pm 12\%$ . The value of  $\alpha$ , with all runs weighted equally, is

$$\alpha(\text{K}) = (36.5 \pm 4.5) \times 10^{-24} \text{ cm}^3.$$

#### 5. Sodium Measurements

Measurements were made on the (2,0) and (2,1) substates of  $\text{Na}^{23}$  at its own zero-moment field ( $H=316$  gauss), and on the (2,-1) state at, or close to, the second zero moment field of  $\text{Rb}^{85}$ . The over-all error is estimated to be  $\pm 13\%$ . The value of  $\alpha$  obtained from the data presented in Table I, with all runs weighted equally, is

$$\alpha(\text{Na}) = (20.0 \pm 2.5) \times 10^{-24} \text{ cm}^3.$$

#### 6. Lithium Measurements

As with potassium, the hyperfine separations for the lithium isotopes are quite small, so that the resolving power of the apparatus was insufficient to separate the substates in the intermediate field region. Unfortunately, it was not practical to work in the high field region since this would have required electric fields in excess of the electrode breakdown field (about 130 000 v/cm) in order to obtain  $E$ - $H$  balance. Determinations for lithium were therefore made without complete separation of the various lithium substates. However, certain of these could be identified by the abrupt changes in slope of the beam intensity vs applied voltage curves. Measurements were made at the zero moment field of  $\text{Na}^{23}$  and also at a field approximately 17% smaller for various lithium substates. Similarly, measurements were made at the same magnetic fields for the rubidium substates for which  $\mu_{\text{eff}} = -\mu_0$ . The quantity  $\alpha(\text{Li})$  was then calculated in terms of  $\alpha(\text{Rb})$ , since

$$\alpha(\text{Li}) = [V(\text{Rb})/V(\text{Li})]^2 (\mu_{\text{eff}}/\mu_0) \alpha(\text{Rb}),$$

where at the particular magnetic field,  $V(\text{Rb})$  and  $V(\text{Li})$  are the applied voltages at the balance condition and  $\mu_{\text{eff}}$  is the effective moment of the lithium substate.

The data for lithium are presented in Table II. The over-all error is estimated to be  $\pm 15\%$  and the value of  $\alpha(\text{Li})$  is

$$\alpha(\text{Li}) = (20.0 \pm 3.0) \times 10^{-24} \text{ cm}^3.$$

TABLE II.  $E$ - $H$  gradient balance measurements for lithium.

Magnetic field (gauss)	$\text{Li}^7$ magnetic substate ( $F, M_F$ )	Effective magnetic moment (Bohr magnetons)	$V(\text{Li})^a$ (kilovolts)	$V(\text{Rb})^b$ (kilovolts)	Lithium polarizability <sup>c</sup> ( $10^{-24} \text{ cm}^3$ )
$\approx 263$	(2,2)	1.0	14.55	10.38	20.4
316 <sup>d</sup>	(2,-1)	0.571	12.23	11.28	19.4
316 <sup>d</sup>	(2,0)	0.743	13.85	11.28	19.7

<sup>a</sup> Average value of applied voltage at balance condition for  $\text{Li}^7$ .

<sup>b</sup> Average value of applied voltage at balance condition for  $\mu_{\text{eff}} = -\mu_0$  substates of rubidium.

<sup>c</sup> Calculated from formula  $\alpha(\text{Li}) = [V(\text{Rb})/V(\text{Li})]^2 (\mu_{\text{eff}}/\mu_0) \alpha(\text{Rb})$ .

<sup>d</sup> Magnetic field corresponding to the zero moment of  $\text{Na}^{23}$ .

TABLE III. Experimental and theoretical determinations of alkali polarizabilities (in units of  $10^{-24}$  cm<sup>3</sup>).

Investigators	Method	Li	Na	K	Rb	Cs
Present experiment	Atomic beam $E$ - $H$ gradient balance method	$20 \pm 3$	$20 \pm 2.5$	$36 \pm 4.5$	$40 \pm 5$	$52.5 \pm 6.5$
Scheffers and Stark <sup>a</sup>	Atomic beam electrostatic deflection method	$12 \pm 0.6$		$34 \pm 1.7$		$42 \pm 2.1$
Fues <sup>b</sup>	Optical Stark effect	27	27	45	50	61
Drechsler and Müller <sup>c</sup>	Field emission microscope measurement	$16 \pm 3$				
Dalgarno and Kingston <sup>d</sup>	Calculations relying upon experimental and theoretical values of oscillator strengths	$24.4 \pm 2.4$	$24.6 \pm 2.5$	$41.6 \pm 4.2$	$43.9 \pm 4.4$	$53.8 \pm 5.4$
Sundbom <sup>e</sup>	Perturbation calculation	20				
Parkinson <sup>f</sup>	Perturbation calculation	25				

<sup>a</sup> See reference 1.<sup>b</sup> See reference 6.<sup>c</sup> M. Drechsler and E. W. Müller, Z. Physik **132**, 195 (1952).<sup>d</sup> See reference 4. The uncertainties for the Dalgarno and Kingston calculations are estimated to be about 10% by Professor Dalgarno (private communication).<sup>e</sup> See reference 3.<sup>f</sup> See reference 5.

## 7. Experimental Error

The largest contribution to the error in our determinations of  $\alpha$  is due to the uncertainty regarding the value of the electric field at the beam position. This uncertainty results largely from the error in location of the beam relative to the pole faces. In our case, this location was essentially determined by the positioning of a collimating slit which was fixed directly onto the pole face assembly. We estimate that the uncertainty in the beam location introduces a possible systematic error in  $E$  of at most 4%. The additional errors introduced by the fringing fields, machining imperfections, warping during heat treatment, and the voltmeter, increase the total estimated error in  $E$  to 5.5%, or an error in  $\alpha$  of 11%.

In almost all cases, the error in the determination of the magnetic field was quite small and random in nature.<sup>6</sup> We estimate the error in  $H$  to raise the over-all error in  $\alpha$  at most by 3%. The errors introduced because of the lack of perfect congruency, and the defocusing effects of the finite beam width can be shown to be insignificant compared to the above errors. The total percentage errors differ slightly for the various alkalis, with the largest error being associated with lithium (see previous section).

## DISCUSSION OF RESULTS

The values of the alkali polarizabilities obtained by our method are listed in Table III, which also summarizes other experimental and theoretical determinations. Our values agree quite well with those of Dalgarno and Kingston, whose calculations rely upon experimental and theoretical values of oscillator strengths for discrete and continuous transitions. The Scheffers and Stark results for lithium and cesium are considerably lower than ours, with the discrepancy probably attributable to the difficulties involved in the analysis of their large shift deflection patterns. Our results agree within the limits of the errors involved (experimental and theoretical) with the other values tabulated, in-

cluding the rather high estimates by Fues for which the uncertainties are probably quite large.

In addition, we have recently been informed that the results obtained by Chamberlain and Zorn are in good agreement with our determinations.<sup>14</sup>

We can conclude from our data that the polarizability values for the various substates of each of the alkalis for which balance measurements were made are the same to within the experimental error. The results of measurements which were made over a range of electric fields for cesium, rubidium, and sodium also show that the polarizabilities are essentially independent of the magnitude of the electric field (up to about 400 esu).

It is believed that the type of apparatus used in these measurements (based on the  $E$ - $H$  gradient balance method) can be quite useful in applications where highly efficient magnetic substate selection is required e.g., the production of beams of polarized ions by ionization of atoms in selected Zeeman substates.

## ACKNOWLEDGMENTS

Both Dr. Joseph Eisinger of Bell Telephone Laboratories, Murray Hill, and Professor Kenneth Rubin of New York University made valuable contributions to the development of the  $E$ - $H$  gradient balance method. We had many stimulating and useful conversations with Drs. G. E. Chamberlain and J. C. Zorn of Yale University. We wish to thank W. Riederer and H. Kufert of the Physics Department machine shop, who constructed a large part of the atomic beam apparatus.

## APPENDIX

### Deviation from Balance Condition Over Width of Beam; Defocusing Conditions; Resolution of Substates

We assume the balance condition to hold along the central line of a beam of finite width traveling parallel

<sup>14</sup> We are indebted to Dr. Chamberlain and Dr. Zorn for informing us of their results prior to publication.

to the pole faces of the  $E$ - $H$  field assembly. Deviations from balance generally occur over the beam width, and we now estimate the resulting defocusing action. We label all quantities along the central line with the subscript 1, and so

$$\mu_1 H_1 = \alpha E_1^2. \quad (\text{A1})$$

At a small transverse distance  $\delta z$ , from the central line ( $z=0$ ), the electric field, magnetic field, and effective moment are given, respectively, to first order by

$$E_1 + (\partial E / \partial z)_1 \delta z, \quad H_1 + (\partial H / \partial z)_1 \delta z, \quad \text{and} \quad \mu_1 + (\partial \mu / \partial z)_1 \delta z.$$

Using the congruency condition  $\partial E / E \partial z = \partial H / H \partial z = C$ , where  $C$  is assumed independent of  $z$  for small  $z$ , and using (A1), the unbalanced force,  $\delta F$ , on a beam atom becomes

$$\delta F = \alpha C E^2 - \mu C H \\ = [2\alpha C E^2 - \mu C H - (\partial \mu / \partial z) H]_1 C \delta z, \quad (\text{A2})$$

where we have neglected second and higher order terms.

Dividing (A2) by the magnitude of either the electric or magnetic force on a beam atom at  $z=0$ , the ratio of the unbalanced force to the electric (or magnetic) force at  $\delta z$  becomes

$$\delta F / F = [1 - (\partial \mu / \partial z) / C \mu]_1 C \delta z.$$

We let  $(\partial \mu / \partial z) = (\partial \mu / \partial H)(\partial H / \partial z)$ , and obtain

$$\delta F / F = [1 - (\partial \mu / \partial H) / (\mu / H)]_1 C \delta z. \quad (\text{A3})$$

Note that a defocusing of the beam occurs if the expression in brackets in (A3) is positive or, equivalently, if

$$(\partial \mu / \partial H)_1 / (\mu / H)_1 < 1. \quad (\text{A4})$$

This inequality was satisfied in most of the balance measurements.

To give an idea of the magnitude of the defocusing action, consider the potassium experiments which were performed under high field conditions for which  $\mu \approx \mu_0$  and therefore  $(\partial \mu / \partial H)_1 \approx 0$ . With a few exceptions, the deviation from balance was smaller in the other alkali measurements since  $(\partial \mu / \partial H)$  was generally positive, and so the potassium deviation can be considered to be an upper limit.<sup>15</sup>

Assume an original beam width of 0.010 cm (a conservative estimate). We therefore substitute  $\delta z = 0.005$  cm in (A3), and assuming  $C = 2.50 \text{ cm}^{-1}$ , we obtain  $\delta F / F = 0.013 = 1.3\%$  as the largest relative force on a beam atom. This corresponds to a deflection in the plane of the detector of about 0.001 in, with the magnetic fields used in the experiment.

<sup>15</sup> It should be recalled that we have consistently referred to  $\mu$  as a *magnitude* throughout our discussion, and therefore the statement  $(\partial \mu / \partial H)_1 < 0$  implies a positive slope for a substate with negative effective moment.

It is interesting to note that in the special case of  $(\partial \mu / \partial H)_1 = (\mu / H)_1$ , the balance condition can be rigorously satisfied for a finite beam, and that a definite focusing of the beam will occur if

$$(\partial \mu / \partial H)_1 / (\mu / H)_1 > 1. \quad (\text{A5})$$

This discussion explains the noticeably different focusing characteristics for the three  $\text{Cs}^{133}$  magnetic substates recorded as balance peaks in Fig. 6. The calculated values of the quantity  $(\partial \mu / \partial H)_1 / (\mu / H)_1$  for the  $(4, -1)$ ,  $(3, -3)$ , and  $(4, 0)$  substates at this field (1634 gauss) are 1.9, -1.8, and 0.8 respectively. It is therefore seen that the very sharp  $(4, -1)$  peak is indeed focusing whereas the attenuated  $(3, -3)$  peak is strongly defocusing. The  $(4, 0)$  substate has weakly defocusing characteristics.

We now derive a criterion for resolution of adjacent magnetic substates, one of which is balanced. The deflection  $S_\alpha$  of a beam atom possessing the most probable oven velocity is  $S_\alpha = GF / (4kT)$ , where  $F$  is the average value of the transverse force on the atom in the region between the pole faces and  $G = l_1^2 + 2l_1 l_2$  (see Fig. 1). We require that  $S_\alpha$  for the unbalanced substate (labeled 2) be considerably greater than  $W/2$  for the undeflected beam, where  $W$  is the width at half-maximum intensity. As a reasonable statement of the resolution criterion, we can say that resolution is achieved if  $S_\alpha > 2(W/2)$ .

Since

$$F_2 = \mu_2 \partial H / \partial z - \alpha E \partial E / \partial z,$$

it follows that

$$C[\mu_2 H - \alpha E^2] > 4kTW / G, \quad (\text{A6})$$

where the  $\mu$ ,  $H$ , and  $E$  values represent averages over the trajectory, which can for the purposes of our calculation be replaced by the values for an undeflected path. Using (A1), we obtain

$$(\mu_2 - \mu_1) / \mu_0 > (4kT / GC\mu_0 H) W.$$

For our apparatus,  $G = 4900 \text{ cm}^2$  and  $C = 2.50 \text{ cm}^{-1}$ , so that

$$(\mu_2 - \mu_1) / \mu_0 > 4.85 (T / H) W, \quad (\text{A7})$$

with  $W$  expressed in centimeters.

As an example of the application of this resolution criterion, consider the recorder traces of Fig. 8 showing the balance peaks of the  $\text{Rb}^{85}$  (3,0),  $\text{Rb}^{85}$  (3,1), and the  $\text{Rb}^{87}$  (2,1) magnetic substates at a magnetic field of 722 gauss. Letting  $W = 0.020$  cm and  $T = 500^\circ \text{K}$ , the resolution criterion becomes  $(\mu_2 - \mu_1) / \mu_0 > 0.07$ . This criterion is certainly satisfied for the  $\text{Rb}^{85}$  (3,0) substate since the adjacent  $\text{Rb}^{87}$  (2,1) substate is higher in effective moment by  $0.12 \mu_0$ . However, the  $\text{Rb}^{87}$  (2,1) and the  $\text{Rb}^{85}$  (3,1) substates differ in effective moment by only  $0.05 \mu_0$ , a difference not great enough to permit resolution.